

Research Article

Cite this article: Varanasi VK, Brabham C, Norsworthy JK (2018) Confirmation and Characterization of Non-target site Resistance to Fomesafen in Palmer amaranth (*Amaranthus palmeri*). *Weed Sci* 66:702–709. doi: 10.1017/wsc.2018.60

Received: 1 May 2018

Revised: 18 July 2018

Accepted: 19 July 2018

Associate Editor:

Christopher Preston, University of Adelaide

Key words:

Cytochrome P450; fomesafen; glutathione S-transferase; GST; *PPX1*; *PPX2*; protoporphyrinogen oxidase

Author for correspondence:

Vijay K. Varanasi, Altheimer Laboratory, 1366 West Altheimer Drive, Fayetteville, AR 72704. (Email: varanasi@uark.edu)

Confirmation and Characterization of Non-target site Resistance to Fomesafen in Palmer amaranth (*Amaranthus palmeri*)

Vijay K. Varanasi¹, Chad Brabham¹ and Jason K. Norsworthy²

¹Postdoctoral Research Associate, Department of Crop, Soil, and Environmental Sciences, University of Arkansas, Fayetteville, AR, USA and ²Professor and Elms Farming Chair of Weed Science, Department of Crop, Soil, and Environmental Sciences, University of Arkansas, Fayetteville, AR, USA

Abstract

Palmer amaranth (*Amaranthus palmeri* S. Watson), a dioecious summer annual species, is one of the most troublesome weeds in U.S. cropping systems. The evolution of resistance to protoporphyrinogen oxidase inhibitors in *A. palmeri* biotypes is a major cause of concern to soybean [*Glycine max* (L.) Merr.] and cotton (*Gossypium hirsutum* L.) growers in the midsouthern United States. The objective of this study was to confirm and characterize the non-target site mechanism in a fomesafen-resistant accession from Randolph County, AR (RCA). A dose-response assay was conducted to assess the level of fomesafen resistance, and based on the GR₅₀ values, the RCA accession was 18-fold more resistant to fomesafen than a susceptible (S) biotype. A TaqMan allelic discrimination assay and sequencing of the target-site genes *PPX2* and *PPX1* revealed no known or novel target-site mutations. An SYBR Green assay indicated no difference in *PPX2* gene expression between the RCA and S biotypes. To test whether fomesafen resistance is metabolic in nature, the RCA and the S biotypes were treated with different cytochrome P450 (amitrole, piperonyl butoxide [PBO], malathion) and glutathione S-transferase (GST) (4-chloro-7-nitrobenzofurazan [NBD-Cl]) inhibitors, either alone or in combination with fomesafen. Malathion followed by (fb) fomesafen in RCA showed the greatest reduction in survival (67%) and biomass (86%) compared with fomesafen alone (45% and 66%, respectively) at 2 wk after treatment. Interestingly, NBD-Cl fb fomesafen also resulted in low survival (35%) compared with the fomesafen-only treatment (55%). Applications of malathion or NBD-Cl preceding fomesafen treatment resulted in reversal of fomesafen resistance, indicating the existence of cytochrome P450- and GST-based non-target site mechanisms in the RCA accession. This study confirms the first case of non-target site resistance to fomesafen in *A. palmeri*.

Introduction

Palmer amaranth (*Amaranthus palmeri* S. Watson) is one of the most troublesome weeds in North America (Van Wychen 2016) and has the capacity to rapidly evolve resistance to herbicides. Resistance to 5-enolpyruvylshikimate-3-phosphate synthase (EPSPS), acetolactate synthase (ALS), and photosystem II (PSII) inhibitors has become widespread (Meyer et al. 2015), and protoporphyrinogen oxidase (PPO) inhibitors (WSSA Group 14) have become a herbicide option for growers interested in controlling *A. palmeri* and waterhemp [*Amaranthus tuberculatus* (Moq.) J. D. Sauer] in soybean [*Glycine max* (L.) Merr.] (Owen and Zelaya 2005; Rousonelos et al. 2012). PPO-inhibiting herbicides prevent the conversion of protoporphyrinogen IX to protoporphyrin IX by the plastid-localized PPO (*PPX2*), a dual-targeting (chloroplast and mitochondria) enzyme in *Amaranthus* species (Dayan et al. 2017; Jacobs and Jacobs 1993; Matringe et al. 1989). However, as with other sites of action (SOAs), repeated use of PPO inhibitors for *A. palmeri* control has resulted in the evolution of resistance to this class of herbicides. PPO-inhibitor resistance in *A. palmeri* was first reported in Arkansas (Salas et al. 2016).

Amaranthus tuberculatus and *A. palmeri* have evolved resistance to herbicides through target-site or non-target site mechanisms, and being closely related, have the propensity to evolve the same resistance mechanisms (Heap 2018; Ma et al. 2013; Nakka et al. 2017a, 2017b; Oliveira et al. 2017). The more common target-site resistance (TSR) mechanism involves a single amino acid change in the target enzyme preventing herbicide binding (Powles and Yu 2010; Tranel and Wright 2002) or could be due to target-site gene amplification or over-expression resulting in the large-scale production of target-site protein by the resistant plant (Gaines et al. 2010). Because of its complex nature, non-target site resistance (NTSR) is poorly understood and is considered a greater threat to herbicide sustainability. In plants, NTSR can

be due to decreased herbicide uptake; reduced herbicide translocation; increased herbicide detoxification (metabolism) due to cytochrome P450 monooxygenases (P450s), glutathione S-transferases (GSTs), or glucosyltransferases; or sequestration into vacuoles (Powles and Yu 2010; Yuan et al. 2007). Out of these, metabolic resistance is the most commonly reported non-target site mechanism (Ma et al. 2013; Yu and Powles 2014). The NTSR mechanisms in weeds have been reported for several herbicides, including acetyl coenzyme A carboxylase, PSII, 4-hydroxyphenylpyruvate dioxygenase (HPPD), EPSPS, and ALS inhibitors (Guo et al. 2015; Han et al. 2016; Kaundun et al. 2017; Ma et al. 2013; Nakka et al. 2017a, 2017b; Preston and Wakelin 2008; Yu et al. 2009).

In the case of PPO inhibitors, resistance has only been reported as a target-site mechanism. The first target-site mechanism conferring PPO-inhibitor resistance was initially reported in *A. tuberculatus* and involved a codon deletion in the *PPX2* gene, resulting in the loss of a glycine residue at the 210th position (Δ G210) of the PPO enzyme (Lee et al. 2008; Patzoldt et al. 2006). The codon deletion was subsequently found in *A. palmeri* (Salas et al. 2016); however, several missense mutations have since been reported. First, an arginine to glycine/methionine at position 128 in the PPO enzyme (R128G/M) was reported to confer PPO-inhibitor resistance (Giacomini et al. 2017). More recently, glycine to alanine (G399A), glycine to glutamic acid (G114E), and serine to isoleucine (S149I) substitutions in the *PPX2* gene were shown to confer broad-spectrum resistance to PPO inhibitors in *A. palmeri* (Rangani et al. 2018). A statewide survey recently conducted in Arkansas revealed widespread fomesafen resistance in *A. palmeri*, and the mechanism was predominantly target-site based (Varanasi et al. 2018). High frequencies of the Δ G210 and R128G mutations were reported (49% and 28% of accessions, respectively) in Arkansas (Varanasi et al. 2018). However, several accessions with no known target-site mutations for fomesafen resistance were found, indicating the presence of an NTSR mechanism. Recently, the mechanism for carfentrazone-ethyl resistance in an *A. tuberculatus* population from Illinois was suggested to be NTSR based (Obenland et al. 2017). However, there are no reports of any NTSR mechanism for PPO inhibitors in *A. palmeri*. The objectives of this study were therefore (1) to confirm the NTSR mechanism in a fomesafen-resistant accession, (2) to determine the level of fomesafen resistance in the putative NTSR accession, and (3) to characterize the NTSR mechanism present in the accession.

Materials and Methods

Plant Materials

The putative resistant accession was originally collected in 2016 from a soybean field in Randolph County, AR (RCA). Throughout this paper, the term "RCA" will be used to refer to the putative resistant accession. To create a homogeneous RCA population, about 200 seedlings of the original accession and a susceptible check (S) were sprayed with fomesafen (Flexstar[®] 1.88 EC, Syngenta, Greensboro, NC) at 395 g ai ha⁻¹. The RCA survivors were allowed to grow and produce seed in the growth chamber. Seed produced from surviving plants was used for conducting cytochrome P450- and GST-inhibitor studies in the greenhouse.

Experiments were conducted in greenhouses located at the Alzheimer Laboratory, University of Arkansas, Fayetteville. In all

the experiments, seeds were germinated in plastic trays (25 cm by 55 cm), and at 1 wk after germination, seedlings at the 1- to 2-leaf stage were transplanted into 50-well plastic trays (25 cm by 55 cm) filled with potting mix (Sunshine[®] premix No. 1, Sun Gro Horticulture, Bellevue, WA). Plants were grown in the greenhouse under a 16-h photoperiod and 35/25 C day/night temperature.

Whole-Plant Fomesafen Dose-Response Experiments

To determine the level of resistance in the RCA accession, seedlings generated in the greenhouse from the field-collected seed lot were treated at the 4- to 6-leaf stage with increasing rates of fomesafen. The following rate structures were used for the RCA and a known susceptible based on the 1X rate of 395 g ai ha⁻¹: 0.06X, 0.12X, 0.25X, 0.5X, 1X, 2X, 4X, 8X, and 0.003X, 0.007X, 0.015X, 0.03X, 0.06X, and 0.12X, respectively. A nonionic surfactant was included at 0.25% v/v in all treatments. Treatments were applied using a research track sprayer equipped with two flat-fan spray nozzles (TeeJet[®] spray nozzles, Spraying Systems, Wheaton, IL) calibrated to deliver 187 L ha⁻¹ of herbicide solution at 269 kPa, moving at 1.6 km h⁻¹. Experiments were conducted three times with 15 plants evaluated per treatment in each run. Aboveground dry biomass was collected at 3 wk after treatment (WAT), and data were expressed as a percentage of the nontreated control. Data were analyzed using the 'drc' package in R v. 3.1.2 (R Development Core Team 2017). The relationship between herbicide rate and aboveground dry biomass was established using a four-parameter log-logistic model (Seefeldt et al. 1995) described as follows:

$$Y = C + \frac{D - C}{1 + \exp\{b[\log(x)] - \log(\text{GR}_{50})\}} \quad [1]$$

where Y is the response (aboveground dry biomass) expressed as a percentage of the nontreated control, C is the lower limit of Y , D is the upper limit of Y , b is the slope of the curve around the GR_{50} (effective herbicide dose for 50% biomass reduction), and x is the herbicide dose. The resistance index (Resistance/Susceptibility [R/S]) was calculated using GR_{50} values.

Screening for Target-Site Resistance in the *PPX* Genes

Young leaf tissue from the survivors of a fomesafen treatment (395 g ai ha⁻¹) were collected in 1.5-ml microfuge tubes (Thermo Fisher Scientific, Waltham, MA) and stored at -80 C until use. Genomic DNA (gDNA) was isolated from the leaves using a modified CTAB (cetyl trimethylammonium bromide) protocol (Doyle and Doyle 1987). The quantity and quality of gDNA was determined with a spectrophotometer (NanoDrop 1000, Thermo Fisher Scientific) and agarose gel electrophoresis.

For RNA, the frozen leaf tissue was homogenized in liquid nitrogen using a prechilled mortar and pestle to prevent thawing. The powdered tissue was transferred to a 1.5-ml microcentrifuge tube, and total RNA was isolated using a TRIzol[®] reagent (Thermo Fisher Scientific). Ribonucleic acid was treated with DNase I enzyme (Thermo Fisher Scientific) to remove gDNA contamination. The isolated RNA was stored at -80 C. The quantity and quality (integrity) of total RNA was determined using a spectrophotometer (NanoDrop 1000, Thermo Fisher Scientific) and agarose gel (1%) electrophoresis. Complementary DNA (cDNA) was synthesized from 1 μ g of the total RNA using a RevertAid First Strand cDNA Synthesis Kit (Thermo Fisher Scientific).

A TaqMan[®] quantitative polymerase chain reaction (qPCR) allelic discrimination assay was conducted to detect the presence

or absence of the Δ G210 and R128G/M mutations in the *PPX2* gene. TaqMan[®] qPCR was performed using a CFX 96 real-time detection system (Bio-Rad, Hercules, CA). For each assay, the qPCR reaction mix (10 μ l) consisted of 2 μ l of GoTaq[®] Flexi buffer (Promega, Madison, WI), 1.2 μ l of 25 mM MgCl₂ (Promega), 0.5 μ l of 10 mM dNTP mix (Promega), 0.5 μ l of primer-probe mix (custom TaqMan[®] SNP genotyping assay, Thermo Fisher Scientific), 0.1 μ l GoTaq[®] Flexi DNA polymerase (Promega), 2 μ l of gDNA (50 to 100 ng μ l⁻¹), and 3.7 μ l of molecular-grade water. The qPCR conditions were 95 C for 3 min, 40 cycles of 95 C for 15 s, and 60 C for 1 min followed by a plate read on every cycle. The Bio-Rad CFX software was used to analyze the qPCR allelic discrimination data expressed in relative fluorescence units (RFUs). The TaqMan primer and probe combinations used for detection of the Δ G210 and R128G/M mutations were previously reported in Giacomini et al. (2017) and Varanasi et al. (2018), respectively.

To validate the TaqMan data and determine whether the RCA accession contained any novel target-site mutation(s), the coding sequences (~1,500 bp) of the *PPX2* and *PPX1* genes were amplified from cDNA, sequenced, and analyzed by comparison with a known susceptible. Primers for *PPX2* and *PPX1* genes were designed using OligoAnalyzer v. 3.1 (IDT SciTools 2017; Integrated DNA Technologies, Coralville, IA), based on the sequence information available for *A. tuberculatus* (DQ386116.1 and DQ386115.1) (Table 1).

PCR was performed in a T100 thermal cycler (Bio-Rad). The 50- μ l reaction consisted of 10 μ l of 5X GoTaq Flexi buffer, 4 μ l of 25 mM MgCl₂, 1 μ l of 10 mM dNTP mix, 0.25 μ l of GoTaq Flexi DNA Polymerase, 1 μ l each of forward and reverse gene-specific primers (Table 1), 2 μ l of cDNA, and 30.75 μ l of nuclease-free water. PCR conditions for amplifying the *PPX2* gene were 95 C for 3 min, 35 cycles of 95 C for 30 s, 52 C for 30 s, and 72 C for 2 min, followed by 72 C for 8 min. The amplifying conditions for the *PPX1* gene were similar, except for the annealing temperature of 55 C. The PCR products were purified using a GeneJet PCR purification kit (Thermo Fisher Scientific), and quantified with a NanoDrop spectrophotometer. The purified PCR products (50 ng ml⁻¹) were sent for Sanger DNA sequencing (Genewiz, South Plainfield, NJ), and the resulting RCA and susceptible *PPX1* and *PPX2* sequences were aligned using MultAlin (Corpet 1988). The sequence data from this study have been submitted to GenBank under accession numbers MH160787 and MH160788, respectively.

An SYBR Green assay was also performed to study the expression of *PPX2* gene in the RCA and S biotypes. Fresh leaf tissue was collected from the RCA biotype 3 d after the fomesafen

treatment (survivors). Similarly, tissue from a known S biotype was collected and stored at -80 C. Total RNA was isolated and cDNA was synthesized using the protocol discussed earlier. The synthesized cDNA was used in a qPCR reaction for measuring the *PPX2* gene expression. The qPCR reaction mix (10 μ l) consisted of 5 μ l of PowerUP SYBR Green mastermix (Applied Biosystems, Waltham, MA), 1 μ l each of forward and reverse primers (5 μ M), 1 μ l of molecular-grade water, and 2 μ l of cDNA. Primers for amplifying the *PPX2* gene were designed based on the *A. tuberculatus* sequence information (DQ386116.1) available online (Table 1). *PPX2* gene expression was normalized using β -tubulin as a reference gene (Godar et al. 2015). The qPCR conditions were 50 C for 2 min, 95 C for 2 min, and 40 cycles of 95 C for 30 s and 59 C for 1 min. A melt-curve profile was included following the thermal cycling protocol to determine the specificity of the qPCR reaction. *PPX2*: β -tubulin expression was determined using the 2 ^{Δ Ct} method, where Ct is threshold cycle and Δ Ct is Ct_{Reference gene (β -tubulin)} - Ct_{Target gene (*PPX2*)}. Gene expression was studied using three biological and three technical replicates.

Metabolic Resistance Screen

To test whether fomesafen resistance in the RCA accession is metabolic in nature, seedlings (4- to 6-leaf stage) were treated with the following cytochrome P450 inhibitors with or without fomesafen: malathion (Hi-Yield[®] Malathion, Hi-Yield Chemical, Bonham, TX) at 1,500 g ai ha⁻¹; piperonyl butoxide (PBO; Exponent[®], MGK, Minneapolis, MN) at 1,500 g ai ha⁻¹; and amitrole (3-amino-1,2,4-triazole, Sigma-Aldrich, St Louis, MO) at 13.1 g ai ha⁻¹. The rates selected for the cytochrome P450 inhibitors were based on the study conducted by Oliveira et al. (2017). All the cytochrome P450 inhibitors were applied 2 h before fomesafen treatment. Additionally, seedlings were treated with the GST inhibitor 4-chloro-7-nitrobenzofurazan (NBD-Cl; Sigma-Aldrich) at 270 g ai ha⁻¹, either alone or in combination with fomesafen. NBD-Cl was applied to seedlings 2 d before fomesafen treatment. The NBD-Cl rate of 270 g ai ha⁻¹ was chosen based on a study conducted in atrazine-resistant *A. tuberculatus* (Ma et al. 2016). A known S biotype (2001) was included as a check and treated with the above P450 and GST inhibitors. Based on the whole-plant dose - response experiments (discussed earlier), a 0.06X fomesafen rate was chosen for the S biotype. The experiment was conducted in three runs, each run consisting of five replications (10 plants replication⁻¹). Above-ground dry biomass (oven-dried at 65 C for 3 d) was collected at 2 WAT and converted into biomass reduction (%) relative to the nontreated control. Additionally, percent survival was calculated

Table 1. Primers used for amplifying and sequencing the two isoforms of the protoporphyrinogen oxidase-coding gene *PPX* in *Amaranthus palmeri*, with the quantitative PCR primers used for measuring *PPX2* gene expression in fomesafen-resistant (from Randolph County, AR) and susceptible biotypes also shown.

Gene	Purpose	5' → 3' primer sequence	Amplicon size —bp—	Temperature —C—
<i>PPX1</i>	Sequencing	F 5'-ATTCTACAATGTCCGCCGAC-3'	1,569	54
		R 5'-TATACACCTCCCAAGGCAACAC-3'		
<i>PPX2</i>	Sequencing	F 5'-TCCATTACCCACCTTTACC-3'	1,590	52
		R 5'-TTACGCGGTCTTCTCATCCAT-3'		
<i>PPX2</i>	Gene expression	F 5'-ATGCTGTGGTTGCTACTGCTCC-3'	178	59
		R 5'-ATAAGAACTCCGAAGCCCTCAAGAG-3'		

based on dead/alive counts of 150 plants (50 plants replication⁻¹) taken at 2 WAT.

ANOVA for biomass reduction (%) and survival (%) was performed using JMP Pro v. 13.1 software (SAS Institute, Cary, NC) after confirming normality and homogeneity of the data. The interaction between treatment and run was not significant; therefore, data for all runs were pooled for subsequent analysis. Fisher's protected LSD test (where $P < 0.05$) was used to separate the means.

Results and Discussion

Fomesafen Dose–Response Assay

Based on whole-plant dose–response studies, the RCA accession was confirmed resistant to the PPO inhibitor fomesafen (Figure 1). The fomesafen rate that caused 50% reduction in the aboveground dry biomass (GR_{50}) of the susceptible biotype was 4.3 g ha^{-1} , whereas for the RCA accession it was 77.8 g ha^{-1} . Thus, based on the GR_{50} values, the resistance index (RCA/S) was estimated to be 18-fold. The level of fomesafen resistance due to $\Delta G210$ deletion in *A. palmeri* was reported to be 21-fold (Salas et al. 2016). A recent study by Brabham et al. (2018) using a homozygous population revealed higher GR_{50} values ($\sim 2,500$) for the $\Delta G210$ genotype, indicating higher levels of fomesafen resistance. A broad range of R/S ratios (3 to 90) have been reported for *A. tuberculatus* and *A. palmeri* biotypes with metabolic resistance to ALS, HPPD, and PSII inhibitors, indicating that levels of NTSR could vary depending on the class of herbicide and weed species under investigation (Guo et al. 2015; Hausman et al. 2011; Kaundun et al. 2017; Ma et al. 2013; Oliveira et al. 2017).

Screening for Target-Site Resistance

In plants, the *PPX* gene exists as two different orthologues, the plastidic *PPX1* and the mitochondrial *PPX2*; both encode a PPO enzyme important for heme and chlorophyll biosynthesis (Beale and Weinstein 1990; Lermontova et al. 1997; Watanabe et al. 2001). To date, all the target-site mutations ($\Delta G210$, R128G/M, G399A, etc.), known to confer PPO-inhibitor resistance in broadleaf weeds have been reported in *PPX2* and not *PPX1* (Giacomini et al. 2017; Patzoldt et al. 2006; Rangani et al. 2018).

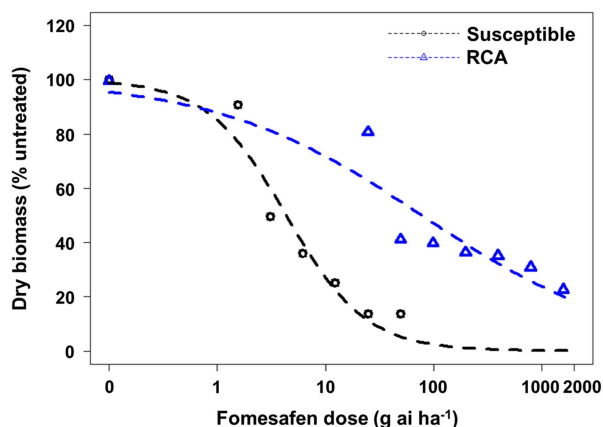


Figure 1. Dose–response assay using four-parameter log-logistic model for the *Amaranthus palmeri* RCA (fomesafen-resistant from Randolph County, AR) and susceptible accessions.

In this study, both *PPX1* and *PPX2* isoforms were analyzed for possible target-site mutations.

A TaqMan qPCR assay to screen for the target-site mutations $\Delta G210$ and R128G/M was conducted on 40 plants from the RCA accession that survived fomesafen at 395 g ai ha^{-1} . The assay revealed no $\Delta G210$ and R128G/M mutations (Figure 2). Furthermore, sequencing of the *PPX2* gene ($\sim 1,500 \text{ bp}$) from five RCA plants and one S plant confirmed the TaqMan results; no known (including G399A, G114E, and S149I; Rangani et al. 2018) or novel mutations conferring PPO-inhibitor resistance were identified (Figure 3). Similarly, no mutations were discovered in the *PPX1* gene of the five RCA plants (unpublished data).

The level of target-site *PPX2* gene expression was analyzed in the RCA and S biotypes using qPCR (Figure 4). No significant difference in *PPX2* gene expression was observed between the RCA and S biotypes, strongly suggesting a non–target site based fomesafen resistance mechanism in the RCA accession.

Cytochrome P450 and GST Inhibitor Assays

The cytochrome P450 inhibitors (malathion, PBO, and amitrole) used in this study are known to target different P450 genes (Oliveira et al. 2017). Increased biomass reduction and herbicide efficacy were observed in HPPD-resistant *A. tuberculatus* when malathion was applied in combination with mesotrione, tembotrione, or topramezone, indicating enhanced metabolism as an NTSR mechanism (Ma et al. 2013; Oliveira et al. 2017). Here, the cytochrome P450 inhibitors followed by (fb) fomesafen treatments showed varied effects on the survival and biomass reduction of the RCA accession (Table 2; Figure 5). PBO and amitrole treatments caused initial injury to the plants; however, the injury was transient, and plants recovered within a week. There were no injury symptoms due to malathion or NBD-Cl application alone. Malathion fb fomesafen resulted in 33% survival rate ($P < 0.05$) and the greatest biomass reduction (86%, $P < 0.05$) when compared with fomesafen applied alone (55% survival and 66% biomass reduction, $P < 0.05$) (Table 2; Figure 6). Similarly,

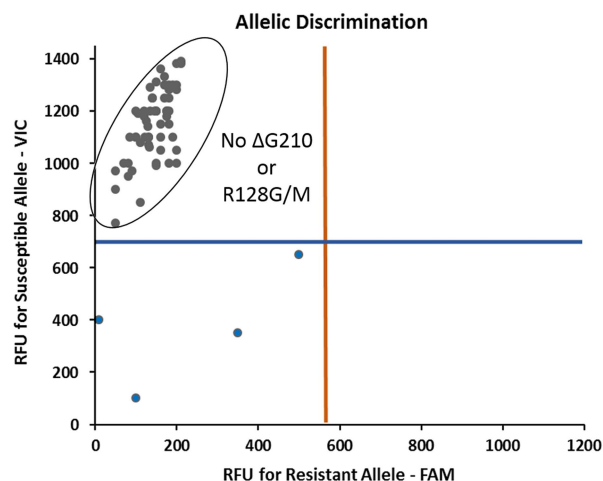


Figure 2. TaqMan quantitative PCR assay for detection of $\Delta G210$ and R128G/M mutations in the *PPX2* gene of the *Amaranthus palmeri* RCA (fomesafen-resistant from Randolph County, AR) biotype. Each of the gray dots at the top left corner of the scatter plot represents an individual plant that survived the field rate of fomesafen (Flexstar[®] at 395 g ha^{-1}). Note the absence of any resistant alleles for $\Delta G210$ and R128G/M mutations. The strength of the amplification signal is measured in terms of relative fluorescence units (RFU). Blue dots at the bottom left indicate no signal from the genomic DNA.

161-1	GTTTTTTTGCAGTTTGTGATTATGTTATTGACCCATTTGTTGCGGGTACATGTGG TGG AGATCCTCAATCGC
161-2	GTTTTTTTGCAGTTTGTGATTATGTTATTGACCCATTTGTTGCGGGTACATGTGG TGG AGATCCTCAATCGC
161-5	GTTTTTTTGCAGTTTGTGATTATGTTATTGACCCATTTGTTGCGGGTACATGTGG TGG AGATCCTCAATCGC
161-10	GTTTTTTTGCAGTTTGTGATTATGTTATTGACCCATTTGTTGCGGGTACATGTGG TGG AGATCCTCAATCGC
161-11	GTTTTTTTGCAGTTTGTGATTATGTTATTGACCCATTTGTTGCGGGTACATGTGG TGG AGATCCTCAATCGC
SUS	GTTTTTTTGCAGTTTGTGATTATGTTATTGACCCATTTGTTGCGGGTACATGTGG TGG AGATCCTCAATCGC
No glycine deletion	
161-1	TTCTGTCACAGCCAATTTACAAAATAAAA AGG TACATAGCTAGAGATGGTCTTCCGGTGCTAGTAAGTCCTC
161-2	TTCTGTCACAGCCAATTTACAAAATAAAA AGG TACATAGCTAGAGATGGTCTTCCGGTGCTAGTAAGTCCTC
161-5	TTCTGTCACAGCCAATTTACAAAATAAAA AGG TACATAGCTAGAGATGGTCTTCCGGTGCTAGTAAGTCCTC
161-10	TTCTGTCACAGCCAATTTACAAAATAAAA AGG TACATAGCTAGAGATGGTCTTCCGGTGCTAGTAAGTCCTC
161-11	TTCTGTCACAGCCAATTTACAAAATAAAA AGG TACATAGCTAGAGATGGTCTTCCGGTGCTAGTAAGTCCTC
SUS	TTCTGTCACAGCCAATTTACAAAATAAAA AGG TACATAGCTAGAGATGGTCTTCCGGTGCTAGTAAGTCCTC
No arginine substitution	

Figure 3. Sequencing of the *PPX2* gene from five fomesafen-resistant (numbered 1, 2, 5, 10, and 11) *Amaranthus palmeri* individuals from the RCA (from Randolph County, AR) accession. Note the absence of Δ G210 (no glycine deletion) and R128G/M (no arginine substitutions) in the *PPX2* gene sequence. cDNA sequences from the resistant plants were compared with a known susceptible (SUS).

applications of PBO or amitrole fb fomesafen caused reductions in biomass (77% and 78%, respectively), even though survival rates (56% and 59%, respectively) were not different from fomesafen alone (Table 2; Figure 5). In contrast, no significant reduction in biomass and survival rates was observed in the S biotype after treatment with P450 inhibitors fb fomesafen (Table 2).

The compound NBD-Cl was shown to cause strong inhibition of the pi class of GSTs expressed in human cancer cells (Ricci et al. 2005) and the phi (F) class of GSTs expressed in herbicide-resistant blackgrass (*Alopecurus myosuroides* Huds.) (Cummins et al. 2013). Interestingly, NBD-Cl fb fomesafen treatment resulted in low survival rate (35%, $P < 0.05$) and reduced biomass by 71%, but the reduction in biomass was not different from fomesafen alone (66%) (Table 2; Figure 7). The lack of biomass reduction could be due to the longer interval (2 d) between the NBD-Cl and fomesafen treatments instead of the 2-h

delay between P450 inhibitors and fomesafen. The low survival rate (35%) after NBD-Cl plus fomesafen application points to a possible role for a GST-mediated mechanism, in addition to the cytochrome P450-based resistance in the RCA accession.

Herbicide metabolism in general involves an activation phase, mediated by cytochrome P450s, followed by a conjugation phase mediated by GSTs (Ghanizadeh and Harrington 2017). Preliminary experiments on treating the RCA accession with both GST and P450 inhibitors preceding the fomesafen application (NBD-Cl + malathion + fomesafen) indicated no increase in control compared with the NBD-Cl or malathion plus fomesafen treatments (unpublished data). Hence, there might not be any additional benefit from mixing both malathion and NBD-Cl with fomesafen to control resistant *A. palmeri*. Further metabolic studies using radioisotopes (^{14}C) are needed to provide more insights into the P450- and GST-based PPO-inhibiting resistance mechanism in the RCA accession.

In summary, this study reports the first documented case of NTSR to fomesafen in *A. palmeri*. The study shows that resistance could partially be reversed by using synergists such as malathion and NBD-Cl, indicating metabolic resistance. It is unknown whether a similar response would be observed under field conditions. Confirmation of these results in the field could lead to better strategies for managing PPO-inhibitor resistance in *A. palmeri*. Use of synergists for reversing herbicide resistance could be one of the tools necessary to counter the growing threat of metabolic resistance in weeds. One of the major reasons attributed to the evolution of metabolic resistance is the use of low or suboptimal rates of herbicides, resulting in the accumulation of metabolic genes over several generations. An important downside of having metabolic resistance in weeds is that it can confer multiple resistance to different chemical families, SOAs, or even compounds that have yet to be commercially developed. Therefore, future studies on the resistance patterns of the fomesafen-resistant RCA accession will be critical to understand the implications of the metabolic resistance.

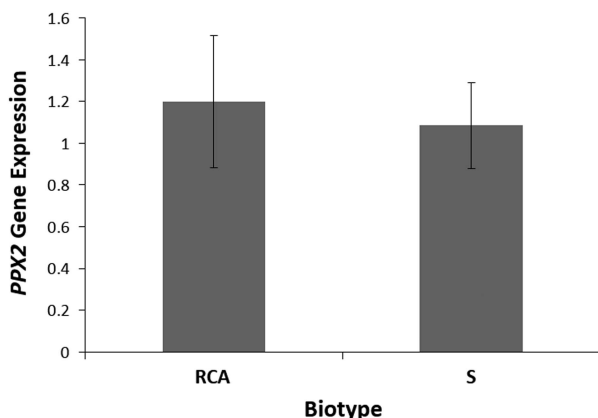


Figure 4. *PPX2* gene expression levels in the RCA (fomesafen-resistant from Randolph County, AR) and susceptible (S) biotypes of *Amaranthus palmeri*. Gene expression was measured relative to the reference gene (β -tubulin). Data represent means of three biological samples, and errors bars represent SE.

Table 2. Effects of cytochrome P450 (malathion, PBO, amitrole) and glutathione S-transferase (NBD-Cl) inhibitors on the percent survival and biomass reduction of the RCA (fomesafen-resistant from Randolph County, AR) and susceptible (S) *Amaranthus palmeri*.^{a,b}

Treatments	Survival ^c (%)	Biomass ^d reduction (%)	Survival ^e (%)	Biomass reduction (%)
	—R—		—S—	
Nontreated control	—	—	—	—
Malathion	100 a	8 a	100 a	10 a
PBO	100 a	14 ab	100 a	1 b
Amitrole	100 a	19 bc	100 a	0 b
NBD-Cl	100 a	25 c	100 a	0 b
Fomesafen	55 b	66 d	70 c	69 c
Amitrole + fomesafen	59 b	78 ef	60 c	70 c
PBO + fomesafen	56 b	77 ef	83 b	66 c
NBD-Cl + fomesafen	35 c	71 de	86 b	44 d
Malathion + fomesafen	33 c	86 f	63 c	71 c

^aAbbreviations: NBD-Cl, 4-chloro-7-nitrobenzofurazan; PBO, piperonyl butoxide.

^bMeans with no common letter(s) within a column are significantly different according to Fisher's protected LSD test, where $P < 0.05$.

^cSurvival % for RCA biotype was calculated based on the dead/alive counts of 150 plants (50 plants replication⁻¹) taken 2 wk after fomesafen and P450- and GST-inhibitor treatments.

^dPercent biomass reduction relative to nontreated control.

^eSurvival % for S biotype was calculated based on the dead/alive counts of 50 plants (10 plants replication⁻¹) taken 2 wk after fomesafen and P450- and GST-inhibitor treatments.



Figure 5. RCA (fomesafen-resistant *Amaranthus palmeri* biotype from Randolph County, AR) plants treated with P450 (amitrole, PBO, malathion) and glutathione S-transferase (NBD-Cl) inhibitors. The treatments included fomesafen (Flexstar[®] at 263 g ai ha⁻¹) alone, amitrole (13.1 g ha⁻¹) followed by (fb) fomesafen, PBO (1,500 g ai ha⁻¹) fb fomesafen, malathion (1,500 g ha⁻¹) fb fomesafen, and NBD-Cl (270 g ai ha⁻¹) fb fomesafen. Amitrole, 3-amino-1,2,4-triazole; NBD-Cl, 4-chloro-7-nitrobenzofurazan; PBO, piperonyl butoxide.

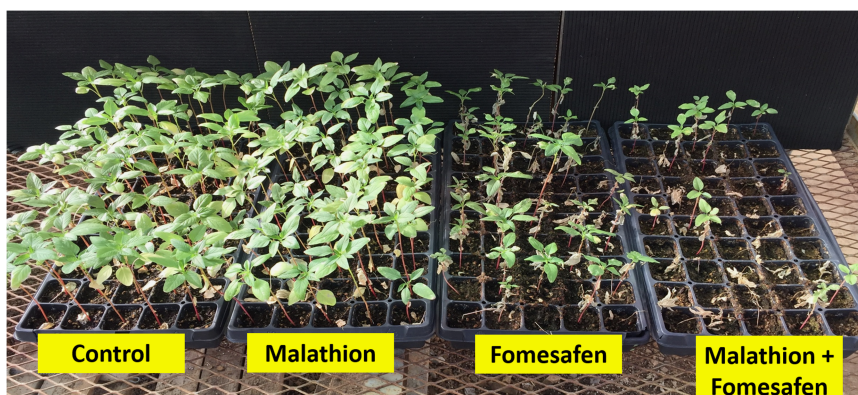


Figure 6. RCA (fomesafen-resistant *Amaranthus palmeri* biotype from Randolph County, AR) plants treated with the P450 inhibitor malathion (1,500 g ha⁻¹), fomesafen (Flexstar[®] at 263 g ha⁻¹), or malathion followed by fomesafen. Picture taken at 2 wk after treatment.

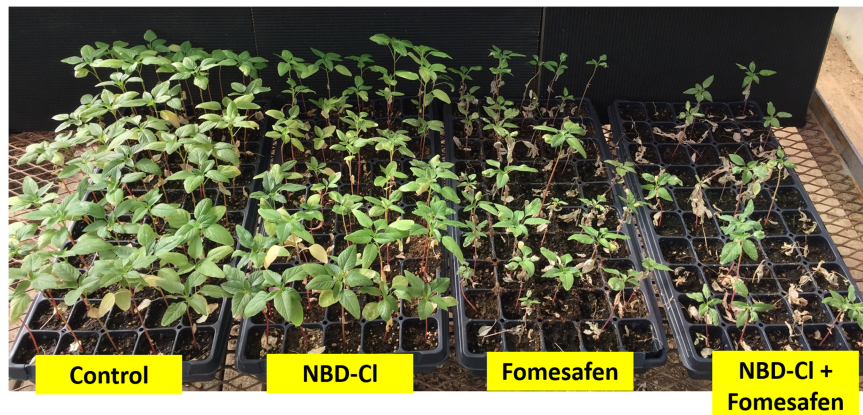


Figure 7. RCA (fomesafen-resistant *Amaranthus palmeri* biotype from Randolph County, AR) plants treated with the glutathione S-transferase inhibitor 4-chloro-7-nitrobenzofurazan (NBD-Cl; 270 g ha⁻¹), fomesafen (Flexstar® at 263 g ha⁻¹), or NBD-Cl followed by fomesafen. Picture taken at 2 wk after treatment.

Acknowledgments. Funding for this research was provided by the Arkansas Soybean Promotion Board. No conflicts of interest have been declared.

References

- Beale SI, Weinstein JD (1990) Tetrapyrrole metabolism in photosynthetic organisms. Pages 287–391 in Dailey HA, ed. Biosynthesis of Heme and Chlorophyll. New York: McGraw-Hill
- Brabham C, Varanasi V, Norsworthy JK (2018) The level of PPO-inhibitor resistance conferred by different mutations in Palmer amaranth. In Proceedings of the 71st Annual Meeting of the Southern Weed Science Society. Atlanta, GA: Southern Weed Science Society of America
- Corpet F (1988) Multiple sequence alignment with hierarchical clustering. *Nucleic Acids Res* 16:10881–10890
- Cummins I, Wortley DJ, Sabbadin F, He Z, Coxon CR, Straker HE, Sellars JD, Knight K, Edwards L, Hughes D, Kaundun SS, Hutchings SJ, Steel PG, Edwards R (2013) Key role for a glutathione transferase in multiple-herbicide resistance in grass weeds. *Proc Natl Acad Sci USA* 110:5812–5817
- Dayan FE, Barker A, Tranel PJ (2017) Origins and structure of chloroplastic and mitochondrial plant protoporphyrinogen oxidases: implications for the evolution of herbicide resistance. *Pest Manag Sci*, doi: 10.1002/ps.4744
- Doyle JJ, Doyle JL (1987) A rapid DNA isolation procedure for small quantities of fresh leaf tissue. *Phytochem Bull* 19:11–15
- Gaines TA, Zhang WL, Wang D, Bukun B, Chisholm ST, Shaner DL, Nissen SJ, Patzoldt WL, Tranel PJ, Culpepper AS, Grey TL, Webster TM, Vencill WK, Sammons RD, Jiang JM, Preston C, Leach JE, Westra P (2010) Gene amplification confers glyphosate resistance in *Amaranthus palmeri*. *Proc Natl Acad Sci USA* 107:1029–1034
- Ghanizadeh H, Harrington KC (2017) Non-target site mechanism of resistance to herbicides. *Crit Rev Plant Sci* 36:24–34
- Giacomini DA, Umphres-Lopez AM, Nie H, Mueller TC, Steckel LE, Young BG, Tranel PJ (2017) Two new PPX2 mutations associated with resistance to PPO-inhibitor herbicides in *Amaranthus palmeri*. *Pest Manag Sci* 73:1559–1563
- Godar AS, Varanasi VK, Nakka S, Prasad PVV, Thompson CR, Jugulam M (2015) Physiological and molecular mechanism of differential sensitivity of Palmer amaranth (*Amaranthus palmeri*) to mesotrione at varying growth temperatures. *PLoS ONE* 10:e0126731
- Guo J, Riggins CW, Hausman NE, Hager AG, Riechers DE, Davis AS, Tranel PJ (2015) Nontarget-site resistance to ALS inhibitors in waterhemp (*Amaranthus tuberculatus*). *Weed Sci* 63:399–407
- Han H, Yu Q, Owen MJ, Cawthray GR, Powles SB (2016) Widespread occurrence of both metabolic and target-site herbicide resistance mechanisms in *Lolium rigidum* populations. *Pest Manag Sci* 72:255–263
- Hausman NE, Singh S, Tranel PJ, Riechers DE, Kaundun SS, Polge ND, Thomas DA, Hager AG (2011) Resistance to HPPD-inhibiting herbicides in a population of waterhemp (*Amaranthus tuberculatus*) from Illinois, United States. *Pest Manag Sci* 67:258–261
- Heap I (2018) The International Survey of Herbicide Resistant Weeds. <http://www.weedscience.org>. Accessed: January 25, 2018
- IDT SciTools (2017) A Suite for Analysis and Design of Nucleic Acid Oligomers. <https://www.idtdna.com/calc/analyzer>. Accessed: September 12, 2017
- Jacobs JM, Jacobs NJ (1993) Porphyrin accumulation and export by isolated barley (*Hordeum vulgare*) plastids. *Plant Physiol* 101:1181–1187
- Kaundun SS, Hutchings S-J, Dale RP, Howell A, Morris JA, Kramer VC, Shivrain VK, McIndoe E (2017) Mechanisms of resistance to mesotrione in an *Amaranthus tuberculatus* population from Nebraska, USA. *PLoS ONE* 12:e0180095
- Lee RM, Hager AG, Tranel PJ (2008) Prevalence of a novel resistance mechanism to PPO-inhibiting herbicides in waterhemp (*Amaranthus tuberculatus*). *Weed Sci* 56:371–375
- Lermontova I, Kruse E, Mock H-P, Grimm B (1997) Cloning and characterization of a plastidal and a mitochondrial isoform of tobacco protoporphyrinogen IX oxidase. *Proc Natl Acad Sci USA* 94:8895–8900
- Ma R, Evans AF, Riechers DE (2016) Differential responses to preemergence and postemergence atrazine in two atrazine-resistant waterhemp populations. *Agron J* 108:1196–1202
- Ma R, Kaundun SS, Tranel PJ, Riggins CW, McGinness DL, Hager AG, Hawkes T, McIndoe E, Riechers DE (2013) Distinct detoxification mechanism confer resistance to mesotrione and atrazine in a population of waterhemp. *Plant Physiol* 163:363–377
- Matringe MJM, Camadro PL, Scalla R (1989) Protoporphyrinogen oxidase as a molecular target for diphenyl ether herbicides. *Biochem J* 260:231–235
- Meyer CJ, Norsworthy JK, Young BG, Steckel LE, Bradley KW, Johnson WG, Loux MM, Davis VM, Kruger GR, Bararpour MT, Ikley JT, Spaunhorst DJ, Butts TR (2015) Herbicide program approaches for managing glyphosate resistant Palmer amaranth (*Amaranthus palmeri*) and waterhemp (*Amaranthus tuberculatus* and *Amaranthus rudis*) in future soybean-trait technologies. *Weed Technol* 29:716–729
- Nakka S, Godar AS, Thompson CR, Peterson DE, Jugulam M (2017a) Rapid detoxification via glutathione s-transferase (GST) conjugation confers a high level of atrazine resistance in Palmer amaranth (*Amaranthus palmeri*). *Pest Manag Sci* 73:2236–2243
- Nakka S, Godar AS, Wani PS, Thompson CR, Peterson DE, Roelofs J, Jugulam M (2017b) Physiological and molecular characterization of hydroxypyruvate dioxygenase (HPPD)-inhibitor resistance in Palmer amaranth (*Amaranthus palmeri* S. Wats.). *Front Plant Sci* 8:555
- Obenland OA, Ma R, O'Brien S, Lygin AV, Riechers DE (2017) Resistance to carfentrazone-ethyl in tall waterhemp. Pages 30–31 in Proceedings of the 72nd Annual Meeting of the North Central Weed Science Society. St Louis, MO: North Central Weed Science Society of America

- Oliveira MC, Gaines TA, Dayan FE, Patterson EL, Jhala AJ, Knezevic SZ (2017) Reversing resistance to tembotrione in an *Amaranthus tuberculatus* (var. *rudis*) population from Nebraska, USA with cytochrome P450 inhibitors. *Pest Manag Sci*, doi:10.1002/ps.4697
- Owen MDK, Zelaya IA (2005) Herbicide-resistant crops and weed resistance to herbicides. *Pest Manag Sci* 61:301–311
- Patzoldt WL, Hager AG, McCormick JS, Tranel PJ (2006) A codon deletion confers resistance to herbicides inhibiting protoporphyrinogen oxidase. *Proc Natl Acad Sci USA* 103:12329–12334
- Powles SB, Yu Q (2010) Evolution in action: plants resistant to herbicides. *Annu Rev Plant Biol* 61:317–347
- Preston C, Wakelin AM (2008) Resistance to glyphosate from altered herbicide translocation patterns. *Pest Manag Sci* 64:372–376
- Rangani G, Salas R, Aponte RA, Landes A, Roma-Burgos N (2018) A novel amino acid substitution (Gly₃₉₉Ala) in protoporphyrinogen oxidase 2 confers broad spectrum PPO-inhibitor resistance in *Amaranthus palmeri*. In Proceedings of the 58th Annual Meeting of the Weed Science Society of America. Arlington, VA: Weed Science Society of America
- R Development Core Team (2017) R: A Language and Environment for Statistical Computing. Vienna, Austria: R Foundation for Statistical Computing. <http://www.R-project.org>. Accessed: December 15, 2017
- Ricci G, De Maria F, Antonini G, Turella P, Bullo A, Stella L, Filomeni G, Caccuri AM (2005) 7-Nitro-2,1,3-benzoxadiazole derivatives, a new class of suicide inhibitors for glutathione S-transferases. Mechanism of action of potential anticancer drugs. *J Biol Chem* 280:26397
- Rousonelos SL, Lee RM, Moreira MS, VanGessel MJ, Tranel PJ (2012) Characterization of a common ragweed (*Ambrosia artemisiifolia*) population resistant to ALS- and PPO-inhibiting herbicides. *Weed Sci* 60:335–344
- Salas RA, Burgos NR, Tranel PJ, Singh S, Glasgow L, Scott RC, Nichols RL (2016) Resistance to PPO-inhibiting herbicide in Palmer amaranth from Arkansas. *Pest Manag Sci* 72:864–869
- Seefeldt SS, Jensen JE, Fuerst EP (1995) Log-logistic analysis of herbicide dose–response relationships. *Weed Technol* 9:218–227
- Tranel PJ, Wright TR (2002) Resistance of weeds to ALS-inhibiting herbicides: what have we learned? *Weed Sci* 50:700–712
- Van Wychen L (2016) 2016 Survey of the Most Common and Troublesome Weeds in Broadleaf Crops, Fruits & Vegetables in the United States and Canada. Weed Science Society of America National Weed Survey Dataset. http://wssa.net/wp-content/uploads/2016_Weed_Survey_Final.xlsx. Accessed: August 10, 2017
- Varanasi VK, Brabham C, Norsworthy JK, Nie H, Young BG, Houston M, Barber T, Scott RC (2018) A statewide survey of PPO-inhibitor resistance and the prevalent target-site mechanism in Palmer amaranth (*Amaranthus palmeri*) accessions from Arkansas. *Weed Sci* 66:149–158
- Watanabe N, Che FS, Iwano M, Takayama S, Yoshida S, Isogai A (2001) Dual targeting of spinach protoporphyrinogen oxidase II to mitochondria and chloroplasts by alternative use of two in-frame initiation codons. *J Biol Chem* 276:20474–20481
- Yu Q, Abdallah I, Han H, Owen M, Powles S (2009) Distinct non-target site mechanisms endow resistance to glyphosate, ACCase and ALS-inhibiting herbicides in multiple herbicide-resistant *Lolium rigidum*. *Planta* 230:713–723
- Yu Q, Powles S (2014) Metabolism-based herbicide resistance and cross-resistance in crop weeds: a threat to herbicide sustainability and global crop production. *Plant Physiol* 166:1106–1118
- Yuan JS, Tranel PJ, Stewart CN Jr (2007) Non-target-site herbicide resistance: a family business. *Trends Plant Sci* 12:6–13